

Comparative Fault Response Study of Synchronous Generator in the Presence of Wind Generator using Singular Perturbation based Transient Stability Index

Sunitha Anup*[‡], Ashu Verma*, T.S.Bhatti*

*Centre for Energy Studies, Indian Institute of Technology, Hauz Khas, New Delhi, India, 110016

(anup.sunitha@gmail.com, averma@ces.iitd.ac.in, tsb@ces.iitd.ac.in)

[‡]Corresponding Author: Tel: +91 9013815364

Received: 20.02.2018 Accepted:27.04.2018

Abstract- The presence of wind generator in interconnected power systems is an important aspect to be considered while studying transient faults. A deeper understanding of transient stability study is essential for the qualitative assessment of the system which includes wind generator. This understanding can be achieved by calculating transient stability index using singular perturbation method. For the calculation of this transient stability index, the state variables are modelled in a realistic approach of slow and fast time frames. In this study, the transient stability assessment results obtained using the method of singular perturbation are compared with the corresponding results calculated using catastrophe theory and linearized singular perturbation methods. In order to understand the implications of presence of a wind generator in the system during transient faults, the study also focuses on the effect of circuit breaker clearing time and generator transient reactance.

Keywords Singular perturbation, transient stability, Lyapunov function, ordinary differential equations, renewable energy.

1. Introduction

Transient stability study is an essential aspect in modern power system, because loss of synchronism in an interconnected power system may lead to cascading failures and blackout of an area in the power grid. It is associated with the ability of the system to withstand large disturbances like three phase fault and loss of generators.

The traditional method of transient stability study is to perform numerical simulations, based on the step-by-step approach [1]. However, this method has certain limitations, some of which are as follows:(a) requirement of smaller step-size poses computational complexity and results in slower convergence,(b) the clearing time is predetermined in the beginning of the solution process. This process has an inherent limitation which could yield inaccurate results due to the ambiguity induced in the predetermination of clearing time, therefore, (c) the method fails to provide a stability limit or index, which is very important to understand how far the disturbance could harm the entire system. The process, however, still remains a reference for the automatic learning methods, since it can be used for training the learning set for pre-analysis study.

An alternative approach of transient stability study is the direct method using energy function formulation. The advantage of energy function formulation over the step-by-step method is that it avoids the repeated iterations which are inevitable in the step-by-step method. The mathematical functions and principles using energy based approaches began for practical power systems about four decades ago. Identification of the appropriate stability region is the most important element in this approach. Different characterizations of stability region and unstable location estimates are widely studied using the energy function approaches namely Closest UEP method, Controlling UEP approach, MOD method, BCU method, PEBS method [2-6].

However, inclusion of detailed modelling of synchronous generator has always remained a challenge in the energy function formulation. Some of the works which have included detailed modelling are given in reference [7]. But the time scaling nature of variables in the power system has not been considered in the above methods. This leads to certain disadvantages like conservative calculation of critical clearing time and computational difficulty in solving the differential equations of the power system model.

To overcome these disadvantages, the problem of stability was studied by factoring time-scaling nature of power system variables. The time scale approach for transient stability was pioneered in a heuristic manner [8]. Thereafter, further work in time-scaling was carried out with decomposition of a large scale power system into slow coherent areas as discussed in references [9]. As far as transient stability is concerned, the modelling of the state variable E'_q is very important. Some of the time-scale models have considered E'_q as either a constant, or a parameter variation or a non-relevant variable. Typically the value of transient time constant of synchronous generator is in the range of 4 to 9 seconds [10] which is more than the clearing time. Thus, to overcome this limitation, it was essential to bring out a mathematical model which considers the coexistence of slow varying variables in the model.

Singular perturbation technique is an ideal nonlinear ordinary differential equation modelling tool, which is capable of modelling the states in different time scales. This technique was carried out for mid-term stability and long term stability studies of the power system as given in reference [11]. In reference [12] transient stability assessment of two time scale power system model using BCU algorithm was done. However, this assessment was based on the requirement of a pseudo fault-on trajectory, which is not applicable for large power system models. The assessment using slow energy function method on a potential energy boundary surface (PEBS) was carried out on a three machine system in reference [12]. The linearized model of singular perturbation was used which is not relevant in a large disturbance scenario. For a single machine infinite bus system, Lyapunov energy function of singularly perturbation model was developed and discussed in [13-22]. It has been observed from the literature review that there are research gaps like consideration of E'_q as slow variable, development of singular perturbation model without linearization and Lyapunov function for multi-machine system using singular perturbation method.

This paper aims to develop a non-linear singular perturbation model of synchronous generator for transient stability study of the multi-machine system. The results of the test system are compared with a similar theory, namely, catastrophe theory, which is an efficient technique in the bifurcation theory for dynamical system. The presence of wind generator in a multi machine system is very relevant in a multi machine system, especially during occurrence of faults. The critical clearing time estimation for a fault is crucial for maintaining the stability of the interconnected power system. This study brings out an efficient and accurate method to obtain the critical clearing time. This is the first time effort to bring singular perturbation and catastrophe theory on the same platform for the study of transient stability of multi machine system. The model also evaluates an index which helps to determine the stability limit.

2. Mathematic Modelling of Multi-machine Power System for Transient Stability

Fig.1 (a) represents a schematic diagram of multi-machine system having n number of generators, r constant impedance loads, having internal voltages of synchronous generators as E_1, E_2, \dots, E_n . The real power injected to the machine is given as

$$P_i = |E_i|^2 Y_{ii} \cos \varphi_{ii} + \sum_{\substack{k=1 \\ k \neq i}}^n |E_i| |E_k| |Y_{ik}| \cos(\varphi_{ik} - \theta_{ik}) \quad (1)$$

P_i is the real power, φ_{ik} is the phase lag between voltage and current vector, Y_{ik} represents the driving point admittances, and if the conductance is neglected, Eq. (1) can be written as

$$P_i = E_i^2 G_{ii} + \sum_{\substack{k=1 \\ k \neq i}}^n E_i E_k G_{ik} \cos(\varphi_{ik} - \theta_i + \theta_k) \quad (2)$$

where, $i = 1, 2, \dots, n$

In Eq. (2), G_{ik} is the real part of reduced Y bus matrix of the system, θ_i is the internal voltage angle. The occurrence of fault in the system results in the change of the Y bus matrix elements.

2.1 Existing model for multi-machine power system [5]

The swing dynamics of an i^{th} generator, with respect to common reference can be given as

$$\frac{2H_i}{\omega_r} \frac{d\omega_i}{dt} + D_i \omega_i = P_{mi} - [E_i^2 G_{ii} + \sum_{\substack{k=1 \\ k \neq i}}^n E_i E_k G_{ik} \cos(\varphi_{ik} - \theta_i + \theta_k)] \quad (3)$$

$$\frac{d\theta_i}{dt} = \omega_i - \omega_r \quad (4)$$

H_i is the inertia coefficient, P_{mi} is the mechanical input power, ω_i, ω_r are absolute machine angle speed and reference speed, D_i is the damping coefficient. Before the occurrence of a large disturbance, the mechanical output and electrical power are balanced and θ_i will have some steady state value. Due to the occurrence of a three phase fault, the electrical power output of the machine reduces to zero and the balance with the mechanical power output is lost, causing acceleration. The behaviour of the angle in Eq. (4) changes with time and the solution of the swing equation determines the stability of the system. Eqs. (3&4) represents the most simplified model of the synchronous generator, namely the classical model. Here, the voltage behind the transient reactance is considered as constant. The electrical dynamics of the rotor is given by,

$$\frac{dE'_{qi}}{dt} = \frac{1}{T'_{doi}} (E_{fd} - E_{qi} + (x_{di} - x'_{di}) I_{di}) \quad (5)$$

where, E'_{qi} , the internal voltage behind transient reactance, is proportional to field flux linkage, T'_{doi} is the direct axis transient time constant, E_{fd} is the excitation voltage and I_{di} is the component of field current in the d-axis, x'_d and x_d are direct axis transient reactance and direct axis reactance respectively. Thus, for an n machine system, there would be $3 \times n$ differential equations in the model. The variation of E'_{qi} in Eq. (5) is expected to be in a slower than the variation of θ_i and ω_i . The dynamics of variables involved in Eq. (5) may be carefully modelled, so that the stability region evaluated in terms of the state variables should be accurate. If all the three state variables are considered in the same time frame, the region would fail to accommodate the dynamics in the appropriate manner. The singular perturbation model incorporates the variation of E'_{qi} in a different time frame using the modelling parameter ε which is reciprocal of the time constant T'_{doi} .

2.2 Modification of the model using singular perturbation

The non-linear equations of a system in singular perturbation model is given by

$$\frac{dx}{dt} = f(x, y) \tag{6}$$

$$\varepsilon \frac{dy}{dt} = g(x, y) \tag{7}$$

where x and y are slow and fast states in the system respectively. ε is the singular perturbation parameter. The above model is represented in singular perturbation modification by considering E'_{qi} as slow state variable and θ_i, ω_i as fast state variables. Fig.1 (b) gives the phasor diagram to illustrate the modified model. $\bar{E}'_{qi}, \bar{\theta}_i$ and $\bar{\omega}_i$ are the stable equilibrium point of non-linear differential equations given in Eqs. (6&7). Using coordinate-transformation, $x_i = E'_{qi} - \bar{E}'_{qi}, y_{1i} = \theta_i - \bar{\theta}_i$ and $y_{2i} = \omega_i - \bar{\omega}_i$, the equilibrium points are shifted to origin. By taking the singular perturbation parameter $\varepsilon = 1/T'_{doi}$, the differential equations changes the time frame from t to t/T'_{doi} . The set of equations can be given as

$$\dot{x}_i = E_{fdi} - \frac{x_e + x_{di}}{x_e + x'_{di}}(x_i + \bar{E}'_{qi}) + (x_{di} - x'_{di})V_i \cos(y_i + \bar{\theta}_i) @f(x, y) \tag{8}$$

$$\varepsilon \dot{y}_{1i} = y_{2i} @g_1(x, y) \tag{9}$$

$$\varepsilon \dot{y}_{2i} = -\frac{\omega_r}{2H_i}(-D_i(y_{2i} + \bar{\omega}_i) + P_{mi} - P_i) @g_2(x, y) \tag{10}$$

The set obtained by putting $\varepsilon = 0$ in Eqs. (6&7), is termed as manifold region, given by

$$y = h(x) \tag{11}$$

The implicit relation gives the algebraic manifold of state variables, geometrically as shown in Fig.1(c). Here, x is a slow variable and two fast variables are y_1 and y_2 . The black solid line shows the exact integral manifold of x as a function of two variables y_1 and y_2 . The incorporation of initial conditions of the variable y in the algebraic expression is made possible with the singular perturbation method using boundary correction factor. Thus, the accuracy remains unaffected by conversion of differential equation to algebraic equation. At the same time, the number of differential equations for an n machine system, is reduced from $3 \times n$ in the existing method to n. When the value of the parameter ε is small, the value of y , obtained by the solution of algebraic equation, approaches the solution of differential equation.

Table 1. Comparison of transient stability investigation using conventional numerical method and singular perturbation method

Method	Conventional numerical integration method	Singular perturbation method
Manifold for stability region	----	$M = \{(x, y) g(x, y) = 0\}$
Accuracy in terms of order of magnitude	No	Yes
Time scale features	No	Yes
Handling issues regarding singularity of the manifold	No	Yes
Classical modelling of synchronous generator	Yes	Yes

2.3 Evaluation of critical clearing angle for post-fault transiently stable multi machine power system using Lyapunov function of the singularly perturbation model

The decomposition of the states using the singular perturbation parameter resulted in decoupling of the system into slow and fast states. This separation in time frame is utilized in formulating a Lyapunov function candidate. The weighted sum of Lyapunov function of the state variables can be given as

$$E = (1 - k)V(x) + kW(x, y) \tag{12}$$

$V(x)$ represents the Lyapunov function for slow states and $W(x, y)$ represents the Lyapunov function of fast states for a small value k. This function is associated with the energy dissipation of the state variables or the stored energy of the state variables in a post fault scenario. It is assumed that y_1

lies in the region $|y_1| \leq \pi - (\sin^{-1}(\frac{\sin \bar{\theta}}{1+x}) + \bar{\theta})$, then E would

be in a decaying mode inside the manifold region defined by Eq. (11). The algebraic equation of this manifold represents the boundary of stability region of the singular perturbation model. The identification of the relevant region of stability is the main requirement for the transient stability study. From the manifold, the unstable equilibrium point can be obtained where the Lyapunov function reaches local minima. The fault on trajectory crosses the stability boundary through the exit point and the critical fault clearing point depends on this exit point. If the exit point matches with the fault clearing point, that fault clearing is considered as critical clearing. The asymptotic stability for the exit point can be obtained from weighted sum of Lyapunov function of slow and fast subsystems. The Lyapunov functions, $V(x)$ and $W(x, y)$ are calculated as follows:

$$V(x) = \int_0^x -f(x, y) dx \tag{13}$$

$$W(x, y) = \frac{D}{2M} (y_1 - h_1(x))^2 + y_2 (y_1 - h_1(x)) + \frac{M}{2D} y_2^2 + \frac{M}{D} (1+x) \int_{h_1(x)}^{y_1} (\sin(y_1 + \bar{\theta}) - \sin(h_1(x) + \bar{\theta})) dy_1 \tag{14}$$

For any small positive value of k , Lyapunov energy function candidates can be obtained for the singular perturbation model. At the exit point, the acceleration of the generator changes sign from negative to positive. If the trajectory of the rotor angle crosses the boundary then the generator would have gained sufficient energy to cross the boundary and would not return to the prefault stable condition. This energy function formulation and identification of critical energy is shown using the well-established equal-area criteria as shown in Fig. 1(d). E_a represents energy function at any location in the manifold. E_a can be positive or negative. The time which corresponds to the critical energy is called the critical clearing time for a fault. A multi-machine system having many machines may be represented by an equivalent two machine system. Also, it is commonly observed that due to disturbance in the system, few generators close to the disturbance swing in unison. Those generators will have same angular velocity during the transient and can be represented by an equivalent generator then the multimachine system becomes a two machine system. The swing equation of the two machines are given as

$$\frac{d^2\theta_1}{dt^2} = \frac{P_{i1} - P_{m1}}{M_1} \tag{15}$$

$$\frac{d^2\theta_2}{dt^2} = \frac{P_{i2} - P_{m2}}{M_2} \tag{16}$$

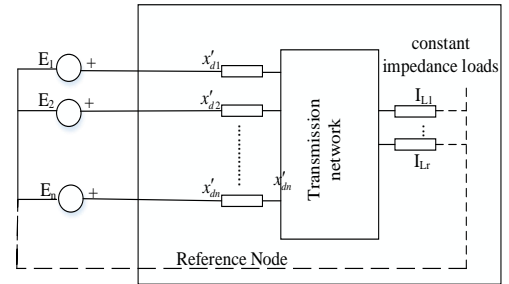
The relative angle $\theta = \theta_1 - \theta_2$ is used to evaluate the stability of two-machine system. M_1 and M_2 are moment of inertia of the machines.

$$\frac{d^2\theta}{dt^2} = \frac{d^2\theta_1}{dt^2} - \frac{d^2\theta_2}{dt^2} = \frac{(P_{i1} - P_{m1})}{M_1} - \frac{(P_{i2} - P_{m2})}{M_2} \tag{17}$$

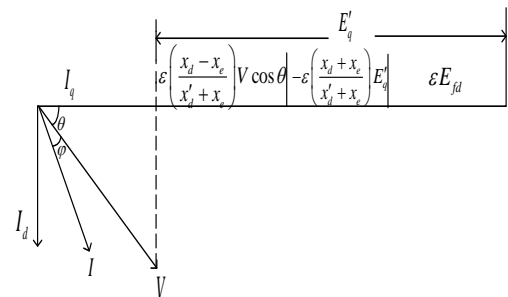
Multiplying either side on Eq. (17) by $M_1 M_2 / (M_1 + M_2)$,

$$\frac{M_1 M_2}{M_1 + M_2} \frac{d^2\theta}{dt^2} = \frac{(M_2 P_{i1} - M_1 P_{i2})}{M_1 + M_2} - \frac{(M_2 P_{m1} - M_1 P_{m2})}{M_1 + M_2} \tag{18}$$

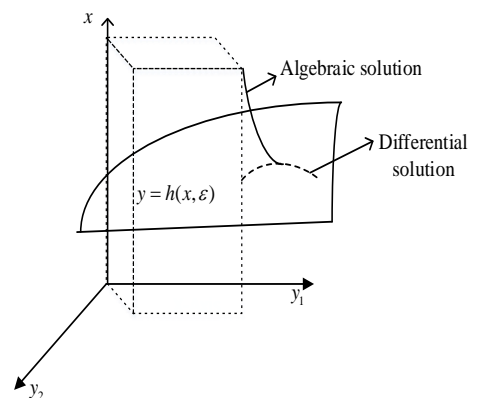
Eq. (18) may be written as, $M \frac{d^2\theta}{dt^2} = P_i - P_{mi}$ (19)



(a)



(b)



(c)

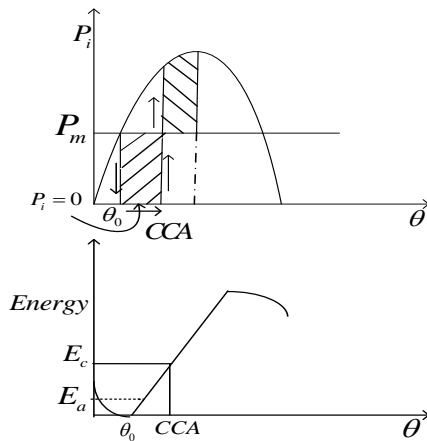


Fig.1. Multi-machine system modelling (a) Schematic diagram, (b) Phasor diagram to illustrate the modification using singular perturbation, (c) Algebraic manifold (d) Power-angle curve and corresponding energy curve according to equal-area criteria

2.4 Evaluation of critical clearing time

During fault the electrical power output reduces to zero and if the fault is cleared within the critical clearing time, accelerating area would be less than or equal to decelerating area. Identifying the critical point/exit point is the important step to determine the critical clearing angle. The critical clearing angle (CCA) is obtained graphically as shown in Fig. 2(a). Using singular perturbation method, the algebraic manifold enables to identify the critical clearing angle. Further, critical clearing time (CCT) can be calculated. The explicit relation of critical clearing angle is given as follows:

$$\frac{d^2 \theta}{dt^2} = \frac{P_m}{M} \tag{20}$$

In Eq. (20), the electrical power $P_i = 0$

Solving Eq. (20) by integrating, we get

$$CCA = \frac{1}{2M} P_m CCT^2 + \theta_0 \tag{21}$$

The critical clearing time can be obtained numerically as

$$CCT = \sqrt{\frac{2M}{P_m} (CCA - \theta_0)} \tag{22}$$

2.5 Formulation of stability index

A quantitative perception of power system transient stability can be obtained by introducing a stability index from the singular perturbation model. The

state variables are presented in the two time scales using the transient time constant, it is more realistic and accurate formulation. The energy of the system Eq. (12) is evaluated at a location/point by using energy function. The critical location is the point where the Lyapunov function based energy reduces to local minima, denoted by E_c . The energy value at any location in the manifold is denoted by E_a . The difference between E_c and E_a gives the stability index given by

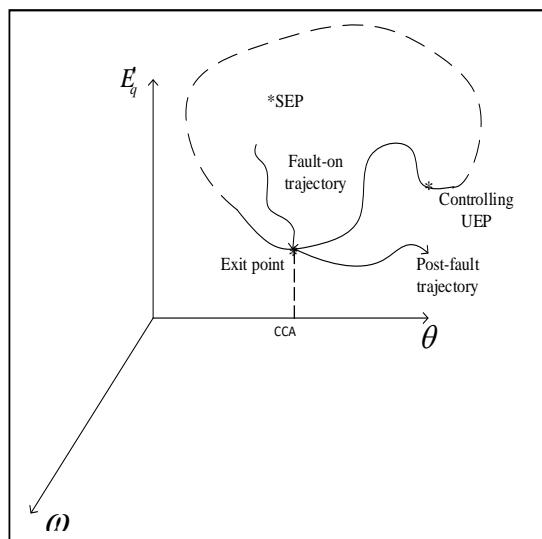
$$StabilityIndex = E_c - E_a \tag{23}$$

The flowchart for evaluation of the stability index is shown in Fig. 2(c).

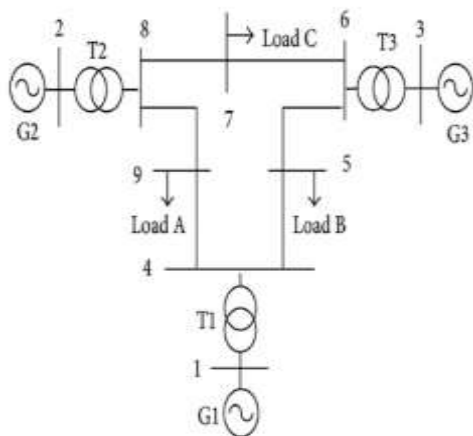
3. Simulation Results

The proposed method is investigated by considering an example of an IEEE three generator, nine bus system, given in Fig.2 (b). The data of the system is given in Appendix-I on 100 MVA base value [14]. Three cases are considered for simulation studies as follows: Case 1 is the classical system with hydro and thermal generators. Case 2 is obtained by replacing generator 3 with wind generator. Case 3 is obtained by replacing generator 1 also by thermal and generator 3 with wind generator as shown in Fig.2.

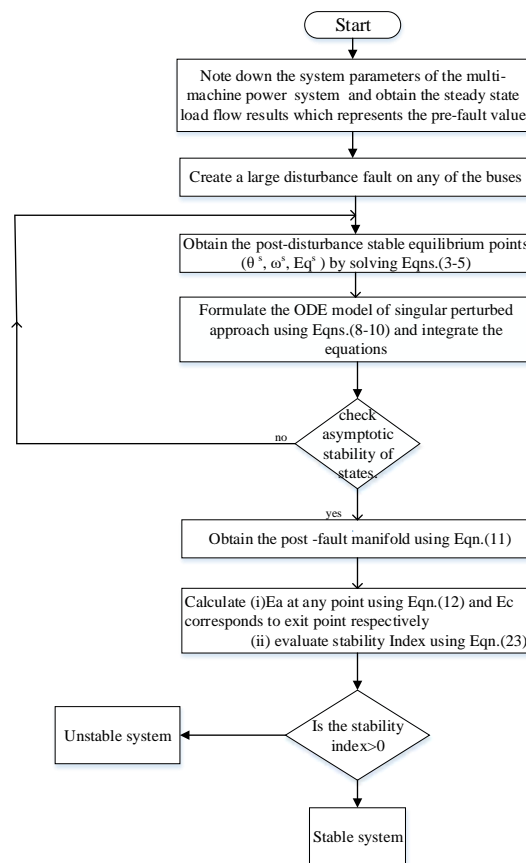
Case 1 represents conventional synchronous generators in the system. The critical clearing time of catastrophe theory method is taken from [14].The singular perturbation method gives a more realistic estimation of critical clearing time as compared to catastrophe theory. It attains importance in generator buses where flux decay modelling gives a more rigorous analysis than classical model. The results of case 1 are also compared with singular perturbation (linearized model) from reference [13] as shown in Table 1.It can be observed that CCT values of non-linear singularly perturbation model is less as compared to linearized singular perturbation model and catastrophe method. It shows that catastrophe method and linearized singular perturbation results are indicating more margin for clearance as these methods have not incorporated rigorous modelling of synchronous generator.. Hence, accurate modelling of generator using non-linear singular perturbation model is required to provide actual critical clearing time.



(a)



(b)



(c)

Fig. 2. Singular Perturbation approach (a) Power system algebraic manifold (b) Test system and cases of studies (c) flow chart for evaluation of stability index

Table 2. Comparison of results of proposed method with singular perturbation model (linearized) and catastrophe method for case 1

Cases	G1	G2	G3
Case 1	Hydro	Thermal	Thermal
Case 2	Hydro	Thermal	Wind,DFIG
Case 3	Thermal	Thermal	Wind,DFIG

3-phase Fault at	CCT using the proposed non-linear singular perturbation model in seconds	CCT using singular perturbation model(linearized)in seconds	CCT using catastrophe method in seconds
Bus 6	0.160	0.180	0.191
Bus 7	0.250	0.295	0.300
Bus 8	0.241	0.251	0.260

One of the synchronous generators, G3 is replaced with DFIG, case 2 and generic model of Power world is used to model DFIG [13]. The parameters used in the study and are given in Appendix II. In case 3, generator G1 is replaced by thermal and generator G3 by DFIG. A comparative study of critical clearing time of the three cases using the proposed methodology is given in Table 2. Introduction of wind energy conversion system in a multi-machine power system has helped in increasing the value of CCT. The larger values of CCT in case2 and

case 3 as compared to case1, are due to the controllers present in DFIG generators. These controllers in the rotor side as well as in the grid side, provides more time for the protective devices to initiate the action of clearance.

Table 3 .Comparison of critical clearing time for test system cases.

3-phase fault at	Case 1 CCT (in seconds)	Case 2 CCT (in seconds)	Case 3 CCT (in seconds)
Bus 1	0.370	0.400	0.420
Bus 2	0.600	0.710	0.730
Bus 3	0.430	0.460	0.550
Bus 4	0.260	0.271	0.280
Bus 5	0.250	0.251	0.270
Bus 6	0.160	0.180	0.175
Bus 7	0.250	0.280	0.295
Bus 8	0.241	0.280	0.279
Bus 9	0.300	0.330	0.370

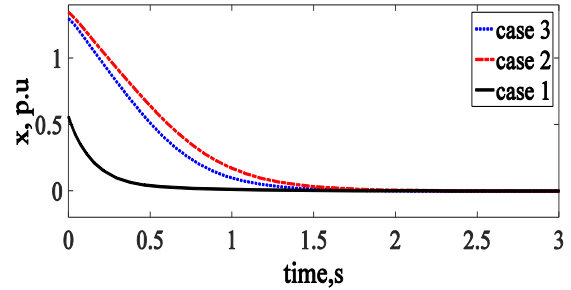
3.2 Effect of circuit breaker (CB) clearing time

The effect of CB clearing time is studied using the singular perturbation approach. If the three phase fault is cleared within the critical clearing time, the system remains stable. A three phase fault event at the generator bus 2 is taken. When the fault is cleared within the critical clearing time, the state variables converge to the stable equilibrium point as shown in Fig.3(a-c). It has been observed that case 1 converges faster than case 2 and case 3. The decaying Lyapunov function for k=0.001 in shown in Fig.3(d).The algebraic manifold of singular perturbation enables to estimate a boundary of region of convergence as shown in Fig.3(e). The initial stable location is marked by point a is shown in Fig.3(e). The critical point marked as point c is btained from the critical point of energy function in Eq.(12). The closest UEP is obtained as the difference of π and stable equilibrium point shown as point b in the Fig.3(e). The comparison of closest unstable equilibrium point(UEP) is given in Table 3.The catastrophe theory considers the stable equilibrium point where the energy function, in case of the classical modelling of synchronous generator,attains null value. The comparison of critical clearing time and critical clearing angle of singular perturbation and catastrophe theory method is shown in Fig.3(f).The time scale separation of the variables of singular perturbation method enables an optimistic value of critical clearing time.The stability index obtained from Eq. (23) for different clearing times is shown in Fig.3(g). Positive value of index represents the stable system and negative value shows unstable system. When the stability index is zero,it represents critically stable system.

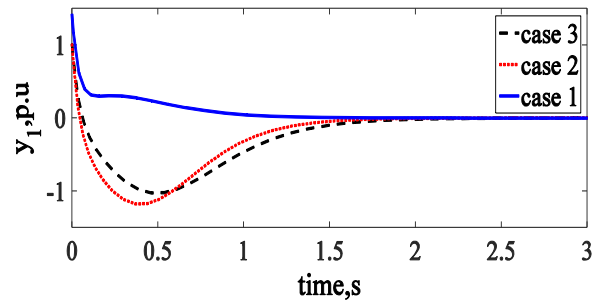
Table 4 .Comparison of equilibrium points of test system cases for three phase fault at G2

Type	Case 1	Case 2	Case 3
SEP,rad	0.608	0.52	0.577

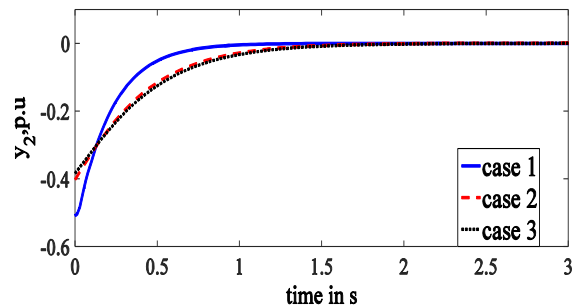
Closest UEP,rad	2.53	2.62	2.56
UEP by singular perturbation	1.5787	1.62	1.73
Manifold	$\sin \theta = \frac{0.560}{E'_q}$	$\sin \theta = \frac{0.570}{E'_q}$	$\sin \theta = \frac{0.600}{E'_q}$



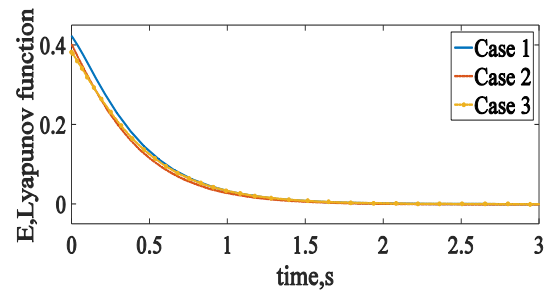
(a)



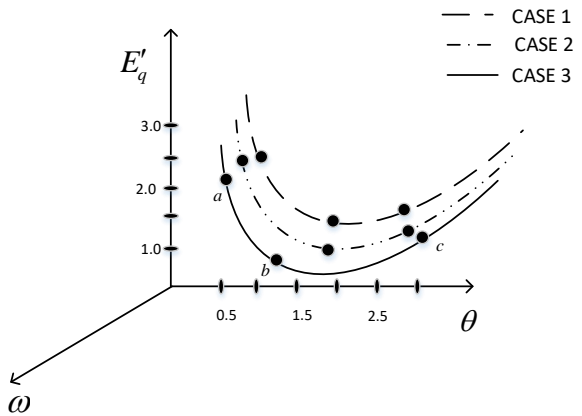
(b)



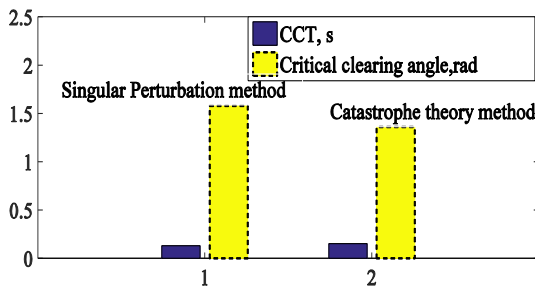
(c)



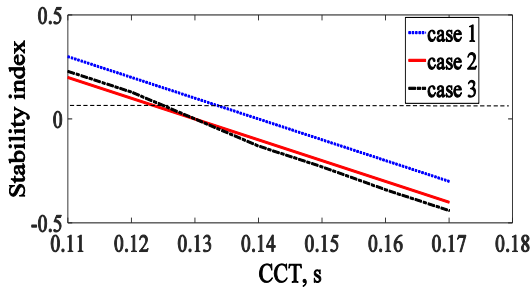
(d)



(e)



(f)



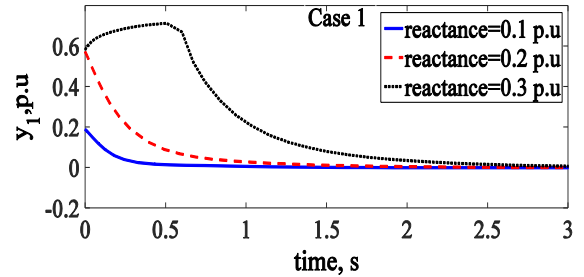
(g)

Fig.3.Asymptotic stability to stable equilibrium point.(a)x,(b)y₁,(c)y₂.(d)Lyapunov function,(e) algebraic manifold for three test cases, (f) comparison of CCT for singular perturbation and catastrophe theory method,(g) comparison of variation of stability indices with respect to critical clearing time for three cases of test system

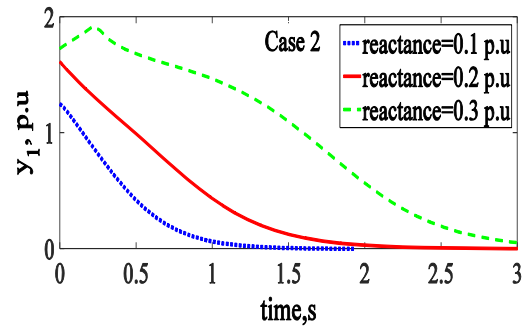
3.3 Effect of system reactance

The generator transient reactance plays a very important role in the transient stability of a system. The event of three phase fault at generator bus 2 is considered. It has been observed that the state variables converge to stable equilibrium point for different transient reactance of generator G2 as seen from Fig.4(a-c).Lower the value of the reactance, faster they converge to the stable equilibrium point. It

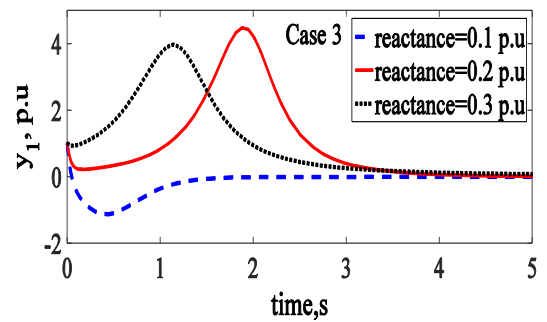
is true for all the test system cases. The comparison of the critical clearing time of test system cases for different transient reactances with the catastrophe theory method is shown in Fig.4(d). The stability index comparison of test system cases for different transient reactances is shown in Fig.4(e).Therefore, it is always advisable to have lower transient reactances of the generators.



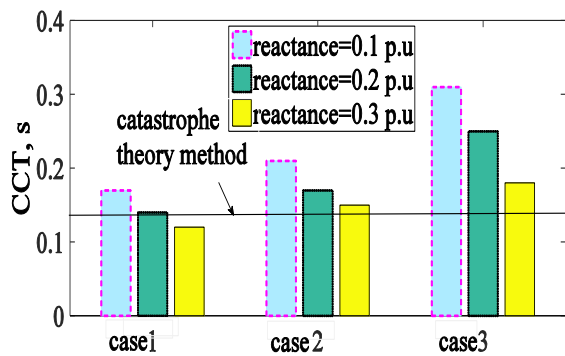
(a)



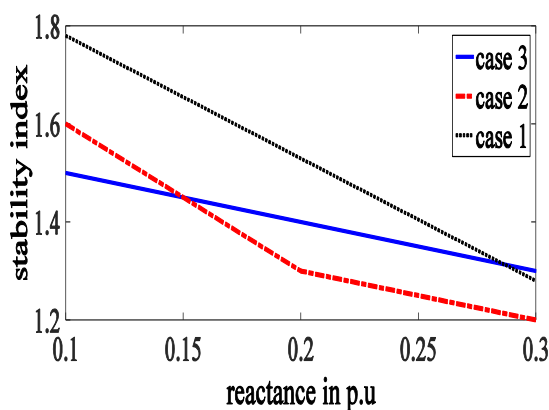
(b)



(c)



(d)



(e)

Fig 4. Asymptotic Stability to the stable equilibrium point, (a) y_1 for case 1, (b) y_1 for case 2, (c) y_1 for case 3, (d) CCT for different values of reactances, (e) stability index for different transient reactances.

4. Conclusion

In this paper, transient stability assessment of power system has been carried out using stability index based on Lyapunov function using singular perturbation method without linearization. The methodology involves

References

[1] Pavella Mania, Damien Ernst and Daniel Ruiz-Vega, Transient stability of power systems: a unified approach to assessment and control, Springer Science & Business Media, 2012. (Book)
 [2] A.A.Fouad and V. Vittal, Power system transient stability analysis using the transient energy function method, Prentice Hall, 1992. (Book)
 [3] H.D.Chiang, Direct methods for stability analysis of electric power systems-theoretical foundation, BCU methodologies and applications, John Wiley & Sons, 2011. (Book)

evaluation of critical clearing angle inside an algebraic manifold to be used for calculating critical clearing time numerically. The stability index obtained using the Lyapunov function identifies critically stable, unstable and stable system from zero, negative and positive values respectively. Singular perturbation model has been developed incorporating the slow dynamics of internal voltage behind transient reactance of a synchronous generator.

The simulation study was conducted on a standard 3-generator, 9 bus power system example to assess the effectiveness and accuracy of the proposed method. Different generator sources, hydro, thermal and wind (DFIG) have been considered for three test system cases to carry out the desired studies. The critical clearing time for 3-phase fault at different buses have been evaluated for comparison. It has been observed that introduction of wind energy conversion system in a multi machine power system has helped in increasing critical clearing time. The controllers in the rotor side and grid side provides more time for the protective devices to initiate the action of clearance. In addition, simulation results of 3-phase bus faults have been compared with that of catastrophe method and linearized singular perturbation method. The modelling of state variables in the singular perturbation model of synchronous generator with correct dynamics ensures a more realistic evaluation of critical clearing time. The effect of circuit breaker clearing time and generator transient reactance have been examined. When the fault has been cleared within the critical clearing time, the system stability has been ensured. The generator reactance is an important parameter which influences the stability of the power system. Lower the value of the reactance, faster the state variables converge to stable equilibrium point. Hence it is advisable to have lower transient reactances of the generator. The stability index developed in this study has been proficient to identify stable and unstable systems. Positive index represents stable system and negative index shows unstable system and when the stability index is zero, it is critically stable system.

[4] Zou, Yun, Ming-Hui Yin, and Hsiao-Dong Chiang, "Theoretical foundation of the controlling UEP method for direct transient-stability analysis of network-preserving power system models", IEEE Trans. on Circuits and Systems I: Funda. Theo. and Appl., Vol 50, No. 10, pp: 1324-1336, 2003. (Article)
 [5] Kundur Prabha, Power system stability and control, Edited by Neal J. Balu, and Mark G. Lauby. Vol. 7. New York: McGraw-hill, 1994. (Book)
 [6] Y. Wu, M. T. Musavi, P. Lerley, B. Conroy, "Prediction of critical generator buses in transient stability using synchrophasor data", Inter. Conf.on Renewable Energy Research and Application (ICRERA), pp. 336-341, 2014.(Conference)

[7] Satpathy Prasanta Kumar, Pradyumna Kumar Sahoo and Mihir Narayan Mohanty, "Elman Neural Network Backpropagation Based Evaluation of Critical Busbars in Power Systems with Renewable Sources", International Journal of Renewable Energy Research (IJRER), Vol 5, No 2, pp: 532-541,2015. (Article)

[8] Avramovic, Bozidar, Petar V. Kokotovic, James R. Winkelman, and Joe H. Chow, "Area decomposition for electromechanical models of power systems", Automatica, No 6, pp: 637-648, 1980. (Article)

[9] Khorasani, K., and M. A. Pai, "Two time scale decomposition and stability analysis of power systems", IEE Proc. D (Control Theory and Applications), Vol. 135, No 3, pp: 205-212, 1988.(Conference)

[10] Vu, Thanh Long, and Konstantin Turitsyn. "Lyapunov functions family approach to transient stability assessment", IEEE Trans. on Power Systems, Vol 31, No 2, pp: 1269-1277, 2016. (Article)

[11] Wright, Sherwin H, "Determination of synchronous machine constants by test reactances, resistances, and time constants", Trans. of the American Insti. of Elec. Engg., Vol.50, No 4 ,pp: 1331-1350, 1931.(Article)

[12] H.D.Chiang and Luís FC Alberto, Stability regions of nonlinear dynamical systems: theory, estimation, and applications. Cambridge University Press, 2015. (Book)

[13] Saberi Ali and Hassan Khalil, "Quadratic-type Lyapunov functions for singularly perturbed systems", IEEE Trans. on Automatic Control, Vol 29, No 6, pp: 542-550,1984.(Article)

[14] Kokotović Peter, Hassan K. Khalil, and John O'reilly, Singular perturbation methods in control: analysis and design, Society for Industrial and Applied Mathematics, 1999.(Book)

[15] Anup Sunitha, Ashu Verma, and T. S. Bhatti, "Transient stability study in solar photovoltaic-wind plant based multimachine system", IEEE Proc. Inter. Conf. Smart Grid and Smart Cities (ICSGSC), pp. 178-182,2017. (Conference)

[16] Demirbas S., R. Bayindir, A. Ova, U. Cetinkaya, and M. Yesil, "Stability analysis of an offshore wind farm connected to turkish electricity transmission system", IEEE Inter. Conf. on Renewable Energy Research and Applications (ICRERA), pp. 314-318 ,2016.(Conference)

[17] Selwa, F., Djamel, L., Imen, L., Hassiba, S. " Impact of PSS and STATCOM on transient stability of multi-machine power system connected to PV generation", Inter. Conf. on Renewable Energy Research and Applications (ICRERA), Palermo, pp. 1416–1421 ,2015.(Conference)

[18] Rekik, Mouna, Achraf Abdelkafi, and Lotfi Krichen, "Synchronization of wind farm power system to utility grid under voltage and frequency variations," Inter. Journal of Renewable Energy Research (IJRER), Vol. 5, No. 1, pp: 70-81, 2015. (Article)

[19] Prasad S, S.C. Tripathy and T. S. Bhatti, "Transient stability analysis of power system using catastrophe theory including field flux decay effect", Electric machines and power systems, Vol 26, pp: 543-464, 1998. (Article)

[20] Baloch, M.H., Wang, J. and Kaloi, G.S., " A review of the state of the art control techniques for wind energy conversion system", Inter.Jour.of Renewable Energy Research (IJRER), Vol 6, No 4, pp.1276-1295. (Article)

[21] Broy, Alexander, Pavlos Touro and Constantinos Sourkounis, "Transient behaviour and active damping of vibrations in DFIG-based wind turbines during grid disturbances", IEEE Inter. Conf. on Renewable Energy Research and Applications (ICRERA), pp. 1405-1410, 2015.(Conference)

[22] Nayir, Ahmet, Eugeniusz Rosolowski and Leszek Jedut, "Analysis of short circuit faults in a system fed by wind turbine", IEEE Inter. Conf. on Renewable Energy Research and Applications (ICRERA), pp. 1-4 ,2012.(Conference)

Appendix

I Test system parameters

Generator	H(s)	x' _d (p.u.)	Transformer reactance(p.u.)	T' _{do} (s)	Rated MVA
Hydro	23.64	0.0608	0.0576	8.96	247.5
Thermal	6.4	0.1198	0.0625	6.00	192.0
Thermal	3.01	0.1813	0.0586	5.89	128.0

Bus	P _g	P _L	Q _L	V
1	0	0	0	1.04
2	1.63	0	0	1.025
3	0.85	0	0	1.025
4	0	0	0	

From Bus	To Bus	Half line charging admittance(p.u.)	Reactance(p.u.)
1	4	0	0.0576
4	6	0.079	0.092
3	9	0	0.0586
6	9	0.179	0.17
5	7	0.153	0.161
7	8	0.0745	0.072
2	7	0	0.0625
8	9	0.1045	0.1008

II DFIG modelling and parameters

The dynamic model of the DFIG is given below. It consists of static model of aerodynamics, a two mass model of drive train, a third order model of generator, AC-DC and DC-AC convertor, pitch controller and converter controller[5]. The rotor of the wind turbine converts the energy from the wind to the rotor shaft. The aerodynamic torque applied to the rotor

by the effective wind speed passing through the rotor is given as

$$T = \frac{\rho}{2\omega_m} A_w c_p (\lambda, \sigma) v_w^3 \tag{24}$$

where, ρ is the air density, ω_m is the wind turbine shaft speed, A_w is the swept area, c_p is the power coefficient, σ is the pitch angle and λ is the tip speed ratio. The drive train attached to the wind turbine transmit the aerodynamic torque T to the high speed shaft. The dynamics of the shaft is given as

$$\dot{\omega}_m = \frac{1}{2H_m} [T - K_s \gamma - D_m \omega_m] \tag{25}$$

$$\dot{\omega}_G = \frac{1}{2H_G} [K_s \gamma - T_e - D_G \omega_G] \tag{26}$$

$$\dot{\gamma} = 2\pi f \left(\omega_m - \frac{1}{N_g} \omega_G \right) \tag{27}$$

where H_m is the inertia constant of wind turbine shaft, H_G is the inertia constant of generator, ω_m is the wind turbine shaft speed, ω_G is the generator speed, K_s is the shaft stiffness, γ is the torsion angle, D is the torsion damping, T_e is the electrical torque, f is the grid frequency and N_g is the gear ratio. The induction generator receives power from the gear box through the stiff shaft. The transient model of DFIG is given as follows [5]:

$$\dot{T}_m = \frac{1}{2H_g} [T_e - T_m] \tag{28}$$

$$\dot{E}'_{qr} = \frac{1}{T'_0} [E'_{qr} - (X - X')] i_{ds} - s \omega_s E'_{dr} - \omega_s v'_{dr} \tag{29}$$

$$\dot{E}'_{dr} = \frac{1}{T'_0} [E'_{dr} + (X - X') i_{qs}] + s \omega_s E'_{qr} + \omega_s v'_{qr} \tag{30}$$

where s is the rotor slip, ω_s is the synchronous speed, T'_0 is the rotor circuit time constant, E'_{qr} and E'_{dr} are the quadrature and direct axis components of transient voltage, X is the rotor open circuit reactance, X' is the transient reactance, v'_{dr} and v'_{qr} are the direct and quadrature axis components of rotor transient voltage.

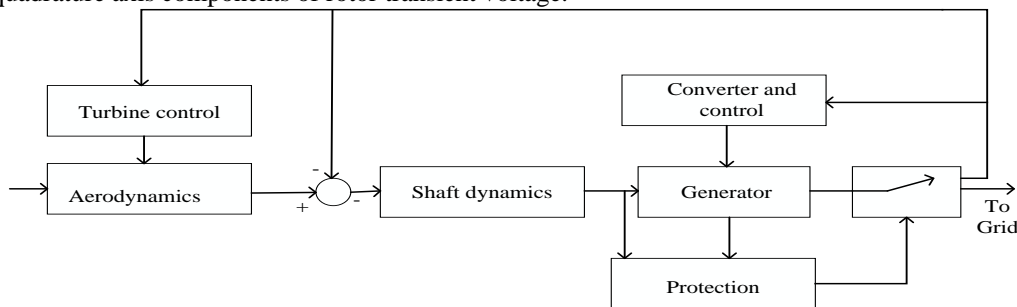


Fig.5.Components of wind generator model

Parameter	Value
-----------	-------

Nominal mechanical output power	0.85 MW
Nominal electrical output power	0.85x0.9 MW
Stator resistance	0.007 p.u.
Leakage inductance	0.17 p.u.
Base frequency	50 Hz
Inertia constant	1 s
Converter control gains	0.3,8
Pitch angle control gains	100,10
Damping Coefficient	1.5 N.m.s